

Injury-stimulated Hedgehog signaling promotes regenerative proliferation of *Drosophila* intestinal stem cells

Aiguo Tian,^{1*} Qing Shi,^{1*} Alice Jiang,¹ Shuangxi Li,¹ Bing Wang,¹ and Jin Jiang^{1,2}

¹Department of Developmental Biology and ²Department of Pharmacology, University of Texas Southwestern Medical Center at Dallas, Dallas, TX 75390

Many adult tissues are maintained by resident stem cells that elevate their proliferation in response to injury. The regulatory mechanisms underlying regenerative proliferation are still poorly understood. Here we show that injury induces Hedgehog (Hh) signaling in enteroblasts (EBs) to promote intestinal stem cell (ISC) proliferation in *Drosophila melanogaster* adult midgut. Elevated Hh signaling by *patched* (*ptc*) mutations drove ISC proliferation noncell autonomously. Inhibition of Hh signaling in the ISC lineage compromised

injury-induced ISC proliferation but had little if any effect on homeostatic proliferation. Hh signaling acted in EBs to regulate the production of Upd2, which activated the JAK–STAT pathway to promote ISC proliferation. Furthermore, we show that Hh signaling is stimulated by DSS through the JNK pathway and that inhibition of Hh signaling in EBs prevented DSS-stimulated ISC proliferation. Hence, our study uncovers a JNK–Hh–JAK–STAT signaling axis in the regulation of regenerative stem cell proliferation.

Introduction

During adult life of multicellular organisms, many organs depend on resident stem cells to maintain tissue integrity by replacing damaged cells, yet the regulatory mechanisms that coordinate stem cell proliferation, self-renewal, and differentiation are still not fully understood. *Drosophila melanogaster* adult midgut has emerged as a powerful system to study stem cell biology in adult tissue homeostasis and regeneration, because of its relatively simple and well characterized cell lineage, similarities to the mammalian intestines, and ease of genetic manipulation of gene activity in this system (Biteau et al., 2011; Jiang and Edgar, 2012).

Drosophila posterior midgut contains self-renewing intestine stem cells (ISCs) located adjacent to the basement membrane of the midgut epithelium (Micchelli and Perrimon, 2006; Ohlstein and Spradling, 2006). ISCs undergo asymmetric cell division to produce renewed ISCs and enteroblasts (EBs), which is controlled by the Par/aPKC/integrin-directed apical–basal cell division and differential BMP signaling that promote asymmetric N signaling essential for the differentiation of ISC daughters

into EBs (Micchelli and Perrimon, 2006; Ohlstein and Spradling, 2006; Goulas et al., 2012; Tian and Jiang, 2014). EBs exit cell cycle and differentiate into either absorptive enterocytes (ECs) or secretory enteroendocrine cells (EEs), depending on the levels of N activity (Ohlstein and Spradling, 2007; Perdigoto et al., 2011; Kapuria et al., 2012). A recent study suggested that EEs are directly derived from ISCs, a process that is controlled by the Slit–Robo signaling pathway (Biteau and Jasper, 2014).

Drosophila midguts undergo slow turnover under normal homeostasis but can mount regenerate programs in response to tissue damage to accelerate stem cell proliferation and differentiation (Amcheslavsky et al., 2009; Jiang et al., 2009). Several signaling pathways, including insulin, JNK, JAK–STAT, EGFR, Wg–Wnt, BMP, Hpo, and Bursicon–DLGR2, have been implicated in the regulation of ISC proliferation during midgut homeostasis and regeneration (Amcheslavsky et al., 2009, 2011; Buchon et al., 2009a; Jiang et al., 2009; Lee et al., 2009; Karpowicz et al., 2010; Ren et al., 2010; Shaw et al., 2010; Staley and Irvine, 2010; Biteau and Jasper, 2011; Jiang et al., 2011;

*A. Tian and Q. Shi contributed equally to this paper.

Correspondence to Jin Jiang: jin.jiang@utsouthwestern.edu

Abbreviations used in this paper: ACI, after clone induction; Ci, Cubitus interruptus; EB, enteroblast; EE, enteroendocrine cell; Hh, Hedgehog; ISC, intestine stem cell; MARCM, mosaic analysis with a repressible cell marker; PH3, phosphohistone 3; Ptc, Patched; Puc, Puckered; Smo, Smoothed.

© 2015 Tian et al. This article is distributed under the terms of an Attribution–Noncommercial–Share Alike–No Mirror Sites license for the first six months after the publication date (see <http://www.rupress.org/terms>). After six months it is available under a Creative Commons License (Attribution–Noncommercial–Share Alike 3.0 Unported license, as described at <http://creativecommons.org/licenses/by-nc-sa/3.0/>).

Xu et al., 2011; Cordero et al., 2012; Guo et al., 2013; Li et al., 2013; Zhou et al., 2013; Scopelliti et al., 2014; Tian and Jiang, 2014). However, how these pathways are regulated in response to tissue damaging and how they are integrated to control stem cell proliferation and differentiation are still poorly understood. Furthermore, it is likely that additional pathways are involved in the regulation of adult midgut homeostasis and regeneration.

Hedgehog (Hh) signaling pathway is one of the major developmental pathways conserved from *Drosophila* to mammals (Jiang and Hui, 2008; Briscoe and Théron, 2013). Hh signaling also plays important roles in the regulation of adult tissue homeostasis and repair in mammals, and its deregulation has been implicated in several types of human cancers (Taipale and Beachy, 2001; Jiang and Hui, 2008; Petrova and Joyner, 2014). However, the mechanism by which Hh signaling is regulated in response to injury, the precise locations where Hh signaling acts, and the downstream effectors that mediate the biological function of Hh signaling have remained largely unexplored. Here, we attempted to address these important questions using *Drosophila* adult midguts as a model system.

Hh exerts its biological function via a conserved signaling cascade (Jiang and Hui, 2008; Briscoe and Théron, 2013). Binding of Hh to its receptor Patched (Ptc) releases the inhibition on the G protein-couple receptor-like seven-transmembrane protein and signal transducer Smoothened (Smo). Activated Smo initiates an intracellular signaling cascade that culminates at the activation of the transcription factor Cubitus interruptus (Ci)/Gli. To explore the role of Hh signaling in *Drosophila* adult midgut homeostasis and regeneration, we used clonal analysis of mutations affecting Hh pathway components including *ptc* and *smo*, as well as tissue-specific RNAi and transgenic overexpression, to alter Hh signaling activity in adult midguts and examined the consequence on normal homeostasis and tissue damage-induced gut regeneration. We found that *ptc* mutant ISC lineage clones over-proliferated compared with the control clones, whereas *smo* mutant clones proliferated normally under homeostatic conditions, and that both *ptc* and *smo* mutant clones differentiated into mature ECs and EEs. Although basal levels of Hh pathway activity in precursor cells did not play a significant role in homeostatic ISC proliferation, Hh signaling was stimulated in response to DSS-induced tissue damage to support regenerative ISC proliferation. Mechanistically, we showed that Hh signaling acted in EBs to promote ISC proliferation by regulating the production of Upd2, which in turn activated the JAK-STAT pathway in ISCs to drive stem cell proliferation. Furthermore, we found that JNK pathway is required for damage-induced Hh pathway activation.

Results

Ptc restricts ISC proliferation in adult midguts

As an initial step to investigate whether Hh signaling plays a role in *Drosophila* adult midgut homeostasis, we generated GFP-labeled homozygous clones for *ptc* or *smo* mutations in 3- to 5-d-old adult females using the mosaic analysis with a

repressible cell marker (MARCM) system (Lee and Luo, 2001). Two *ptc* alleles, *ptc^{lww}* (a null allele) and *ptc^{S2}* (a strong allele), and *smo³* (a null allele) were used. After clone induction, adult flies were cultured at 18°C for certain periods of time before midguts were dissected for immunostaining. 10 d after clone induction (ACI), the majority of the control ISC lineage clones in the posterior region of midguts contained three to five cells whereas the majority of *ptc* mutant ISC lineage clones contained more than five cells (Fig. 1, A–C' and E). Of note, we only included ISC lineage clones in the posterior region of midguts for quantification because of the regional difference in ISC proliferation rate (Buchon et al., 2013; Marianes and Spradling, 2013). The observed increase in clone size suggests that *ptc* mutant clones proliferated faster than the control clones, a notion that was confirmed by examining the mitotic index in midguts carrying *ptc* mutant clones or in which *ptc* was inactivated by RNAi (see results in Fig. 3).

In *Drosophila* Hh signaling pathway, the kinesin-like protein Costal2 (Cos2) inhibits Hh signaling by promoting the phosphorylation and proteolytic processing of Ci into a truncated repressor form and by sequestering the full-length Ci in the cytoplasm; as a consequence, loss of Cos2 leads to Hh pathway activation similar to loss of Ptc (Wang et al., 2000; Zhang et al., 2005). We found that ISC lineage clones homozygous for a strong allele of *cos2* (*cos2²*) also exhibited increased clone size compared with the control clones (Fig. 1, D and E), lending further support to the notion that ectopic Hh pathway activation drives excessive ISC proliferation. Immunostaining with markers for differentiated cells indicated that *ptc* or *cos2* mutant ISC lineage clones contained Pdm1⁺ (an EC-specific marker) and Pros⁺ (an EE-specific marker) cells (Fig. S1), suggesting that ectopic Hh pathway activation promotes the proliferation of ISCs but does not prevent their differentiation into mature cells.

We also compared the size of *smo* mutant clones with that of control clones at 10 or 20 d ACI and found no significant difference between them (Fig. 1, F–K). Collectively, these results suggest that basal Hh signaling activity is not required in ISCs to maintain their homeostatic proliferation but elevated Hh pathway activity, as seen in *ptc* or *cos2* mutant clones, leads to excessive ISC proliferation.

Hh signaling activity is required for regenerative ISC proliferation

We next examined whether Hh pathway activity is required for regenerative proliferation of ISC in response to tissue damage. To block Hh signaling in midgut precursor cells, we knocked down Smo or Ci by expressing *UAS-Smo^{RNAi}* or *UAS-Ci^{RNAi}* using the *esg-Gal4 tub-Gal80^{ts}* (*esg^{ts}*) system in 2- to 3-d-old adult females for 8 d. A *UAS-GFP* transgene was coexpressed with the RNAi transgenes to mark the precursor cells. Both control and RNAi flies were fed with tissue-damaging reagents such as DSS and bleomycin for one day, followed by immunostaining with an antibody against phospho-histone 3 (PH3) to examine ISC proliferation. In line with our previous findings (Amcheslavsky et al., 2009; Ren et al., 2010, 2013), feeding control guts (*esg^{ts}>GFP*) with DSS or bleomycin resulted in

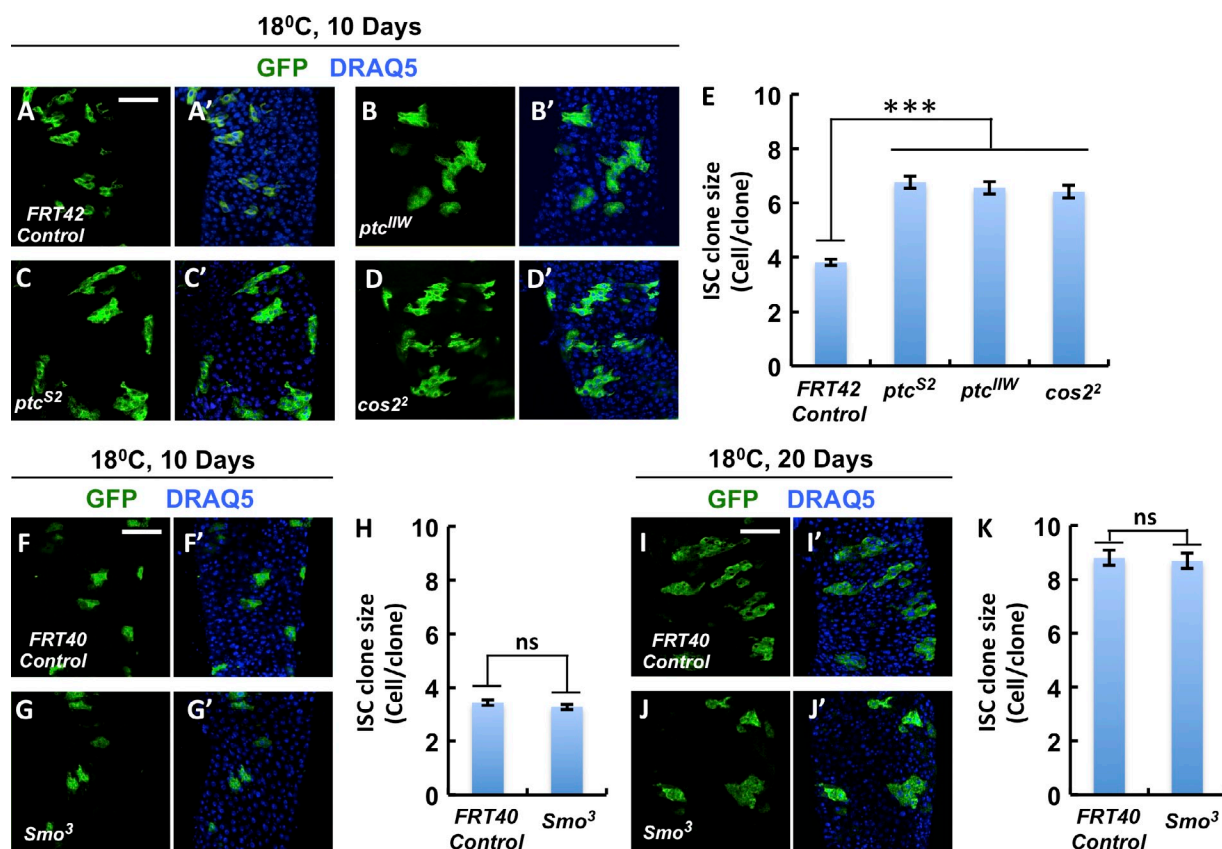


Figure 1. Ptc restricts ISC proliferation in *Drosophila* adult midgut. (A–K) 3- to 5-d-old adult female flies were heat shocked at 37°C for 1 h to induce MACRM clones for control FRT chromosomes (A, A', F, F', I, and I'), *FRT42 ptc^{llw}* (B and B'), *FRT42 ptc^{S2}* (C and C'), *FRT42 cos2²* (D and D'), or *FRT40 smo³* chromosome (G, G', J, and J') and cultured at 18°C for 10 (A–H) or 20 d ACI (I–K). Midguts were immunostained for GFP (green) and DRAQ5 (blue) and clone size was quantified for each genotype (E, H, and K). Clones were marked by GFP and nuclei were marked by DRAQ5. Only ISC lineage clones in the posterior region of midguts were included for quantification. Bars, 50 μ m. Data are mean \pm SEM. $n = 150$. ***, $P < 0.001$. ns, not significant.

elevated ISC proliferation, as indicated by an increase in the number of mitotic cells labeled by the PH3 antibody (Fig. 2, A–C and J). We found that DSS-induced ISC proliferation was nearly abolished by blocking Hh pathway activity in the precursor cells as *esg^{ts}>Smo^{RNAi}* or *esg^{ts}>Ci^{RNAi}* midguts exhibited greatly reduced PH3⁺ cells compared with control guts (Fig. 2, D–E, G–H, and J). Bleomycin-induced ISC proliferation was also affected by Smo or Ci inactivation but to a lesser extent (Fig. 2, F, I, and J). Consistent with reduced ISC proliferation, both *esg^{ts}>Smo^{RNAi}* and *esg^{ts}>Ci^{RNAi}* midguts contained reduced number of *esg>GFP⁺* cells compared with the control guts after DSS treatment (Fig. 2, E and H, compared with Fig. 2 B).

In contrast to perturbation of Hh pathway in precursors, inactivation of Hh signaling in ECs by expressing *UAS-Smo^{RNAi}* using EC-specific Gal4 driver *Myo1A tub-Gal80^{ts}* (*Myo1A^{ts}*) or in visceral muscle cells using visceral muscle-specific Gal4 driver *How tub-Gal80^{ts}* (*How^{ts}*) did not affect either DSS- or bleomycin-induced ISC proliferation (unpublished data), suggesting that Hh pathway activity is required in the precursor cells to support regenerative ISC proliferation in response to tissue damage.

To further explore the role of Hh signaling in midgut regeneration, we used the *esg^{ts}F/O* (*esg-Gal4 tub-Gal80^{ts} UAS-GFP; UAS-flp Act>CD2>Gal4*) system in which all cells in the ISC lineage were labeled by GFP after shifting temperature to

29°C (Jiang et al., 2009). Feeding adult flies with DSS induced a rapid turnover of midgut epithelia, as shown by the newly formed ECs (GFP⁺ Pdm1⁺) and EEs (GFP⁺ Pros⁺) as well as more EBs (GFP⁺LacZ⁺) 1 d after treatment (Fig. 2, L, N, and S). In contrast, mock-treated guts mostly contained GFP⁺ precursor cells at this stage (Fig. 2, K, M, and S). DSS-induced ISC proliferation and epithelial turnover were blocked by inactivation of Hh signaling because rare GFP⁺ ECs or EEs and reduced number of EBs (GFP⁺LacZ⁺) were found in midguts expressing *esg^{F/O}>Smo^{RNAi}* (Fig. 2, P, R, and S).

Hh signaling regulates ISC proliferation noncell autonomously

To further explore the role of Hh signaling in the regulation of regenerative ISC proliferation, we fed adult flies containing *smo³* clones or control clones in midguts with DSS at 5 d ACI. Compared with mock treatment, control ISC lineage clones exhibited increased clone size after DSS treatment (Fig. 3, A–B' and E). Surprisingly, *smo³* lineage clones also exhibited increased clone size in response to DSS treatment compared with sucrose treatment (Fig. 3, C–E). Quantification of the clone size of many clones revealed no significant difference in the average clone size between *smo³* and control clones either in the absence or presence of DSS treatment (Fig. 3 E). Staining with the PH3 antibody revealed that midguts containing *smo³* clones or

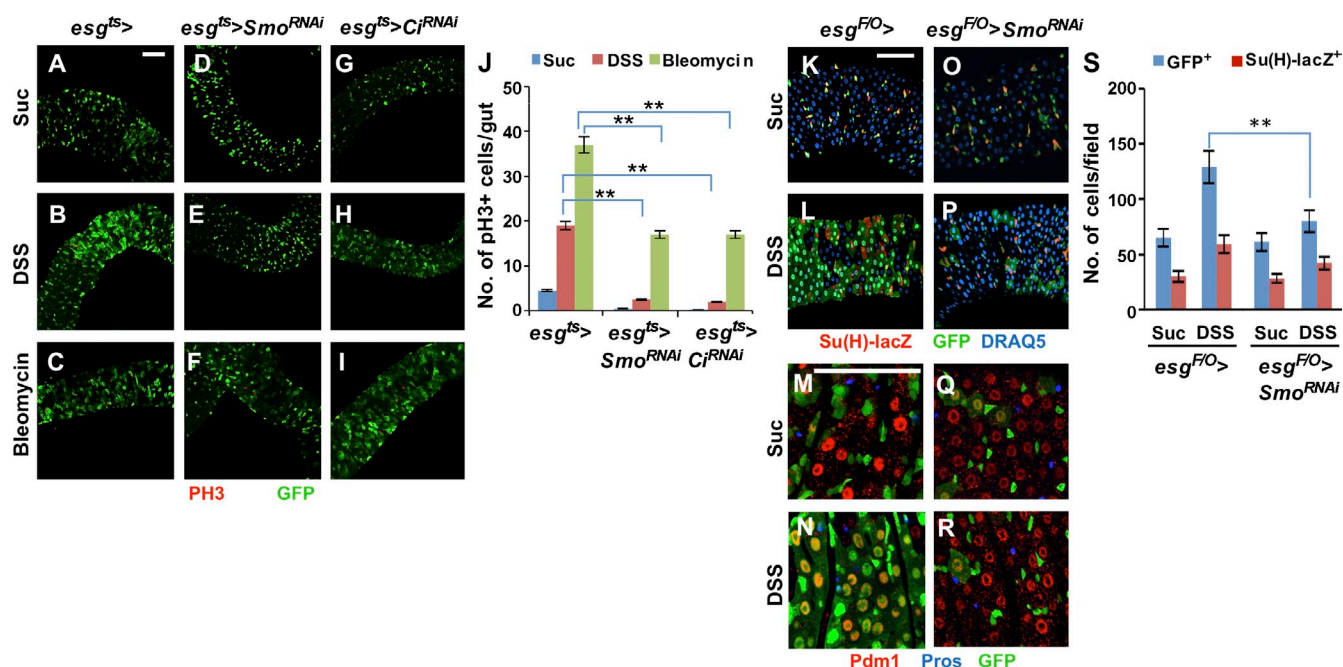


Figure 2. Hh signaling is required in precursor cells for injury-induced ISC proliferation and midgut regeneration. (A–I) 2- to 3-d-old adult females of *esg^{ts}* without (A–C) or with *UAS-Smo^{RNAi}* (D–F) or *UAS-Ci^{RNAi}* (G–I) were shifted to 29°C for 8 d and then treated with Suc, DSS, and bleomycin for 1 d, followed by immunostaining for GFP and PH3. (J) Quantification of PH3+ cells in midguts from adults of the indicated genotypes. Three independent experiments were performed and 12 guts were examined for each sample. Error bars are standard deviations. **, $P < 0.01$. (K–R) 3- to 5-d-old adult females of *esg^{F/O}* without (K–N) or with *UAS-Smo^{RNAi}* (O–R) were shifted to 29°C for 8 d and treated with Suc or DSS for 1 d, followed by immunostaining for GFP and lacZ (K, L, O, and P) or GFP, Pdm1, and Pros (M, N, Q, and R). (S) Quantification of GFP+ or Su(H)-lacZ+ cells in midguts of the indicated genotypes treated with Suc or DSS for 1 d. $n = 20$ for each genotype. Error bars are standard deviations. **, $P < 0.01$. Bars, 50 μ m.

control clones exhibited a similar mitotic index both inside and outside the clones (Fig. 3, B, D, and F). These results suggest that Hh pathway activity is not required in ISCs to support regenerative proliferation and thus point to a noncell-autonomous role of Hh signaling in the regulation of ISC proliferation.

To further explore the noncell-autonomous role of Hh signaling in the regulation of ISC proliferation, we examined PH3 expression in adult midguts carrying *ptc* mutant clones. We observed an increased number of PH3+ cells both within and outside *ptc* mutant clones (Fig. 3, G–I). Quantification of the PH3+ cells indicated that the majority of PH3+ cells were located outside the *ptc* mutant clones (Fig. 3 J). This noncell-autonomous effect suggests that *ptc* mutant cells may secrete a growth factor that acts in a paracrine fashion to stimulate ISC proliferation.

Hh signaling acts in EBs to promote ISC proliferation

To determine where Hh signaling acts to regulate ISC proliferation, we depleted Ptc in different cell types of adult midguts by expressing *UAS-Ptc^{RNAi}* using cell type-specific Gal4 drivers. We found that knockdown of Ptc in ECs by expressing *Myo1A^{ts}>Ptc^{RNAi}* or in ISCs by expressing *Delta(Dl)-Gal4 tub-Gal80^{ts}/UAS-Ptc^{RNAi}* (*DI^{ts}>Ptc^{RNAi}*) failed to increase the number of PH3+ cells (Fig. 3 K). In contrast, knockdown of Ptc in EBs by expressing *Su(H)-Gal4 tub-Gal80^{ts}/UAS-Ptc^{RNAi}* (*Su(H)^{ts}>Ptc^{RNAi}*) increased the number of PH3+ cells (Fig. 3, L–N), suggesting that excessive Hh signaling in EBs promoted ISC proliferation. As a further support of this notion, we found that expression of an active form of Ci that lacks the N-terminal

repressor domain (*Ci^{ΔN}*) in EBs (*Su(H)^{ts}>Ci^{ΔN}*) but not in ISCs (*DI^{ts}>Ci^{ΔN}*) increased the number of PH3+ cells (Fig. 3, O–S).

The observation that DSS stimulated the proliferation of ISCs in *smo* mutant clones but not in midguts expressing *esg^{ts}>Smo^{RNAi}* also implied that Hh pathway activity is required in EBs but not in ISCs to support regenerative proliferation. To determine where Hh pathway activity is required for regenerative proliferation of ISCs, we inactivated Smo in EBs (*Su(H)^{ts}>Smo^{RNAi}*) or ISCs (*DI^{ts}>Smo^{RNAi}*). We found that blocking Hh signaling in EBs but not in ISCs inhibited DSS-induced ISC proliferation (Fig. 3, T–X; and not depicted), demonstrating that Hh signaling acts nonautonomously to regulate ISC proliferation during regeneration.

Hh signaling regulates the production of the JAK-STAT pathway ligand Upd2

To determine the mechanism by which Hh signaling nonautonomously regulates ISC proliferation, we sought to identify the secreted factors regulated by Hh signaling in EBs. It has been shown that ligands of the JAK-STAT and EGFR pathways are up-regulated in response to tissue damage (Jiang and Edgar, 2009; Jiang et al., 2009; Ren et al., 2013; Zhou et al., 2013). Therefore, we used RT-qPCR to examine the expression of these ligands in midguts in which Hh signaling is activated in EBs. We found that the expression of the JAK-STAT pathway ligand Upd2 was significantly induced by overexpression of the active form of Ci (*Su(H)^{ts}>Ci^{ΔN}*) or knockdown of Ptc in EBs (*Su(H)^{ts}>Ptc^{RNAi}*), whereas the expression of other JAK-STAT pathway ligands, including Upd and Upd3, as well as EGFR

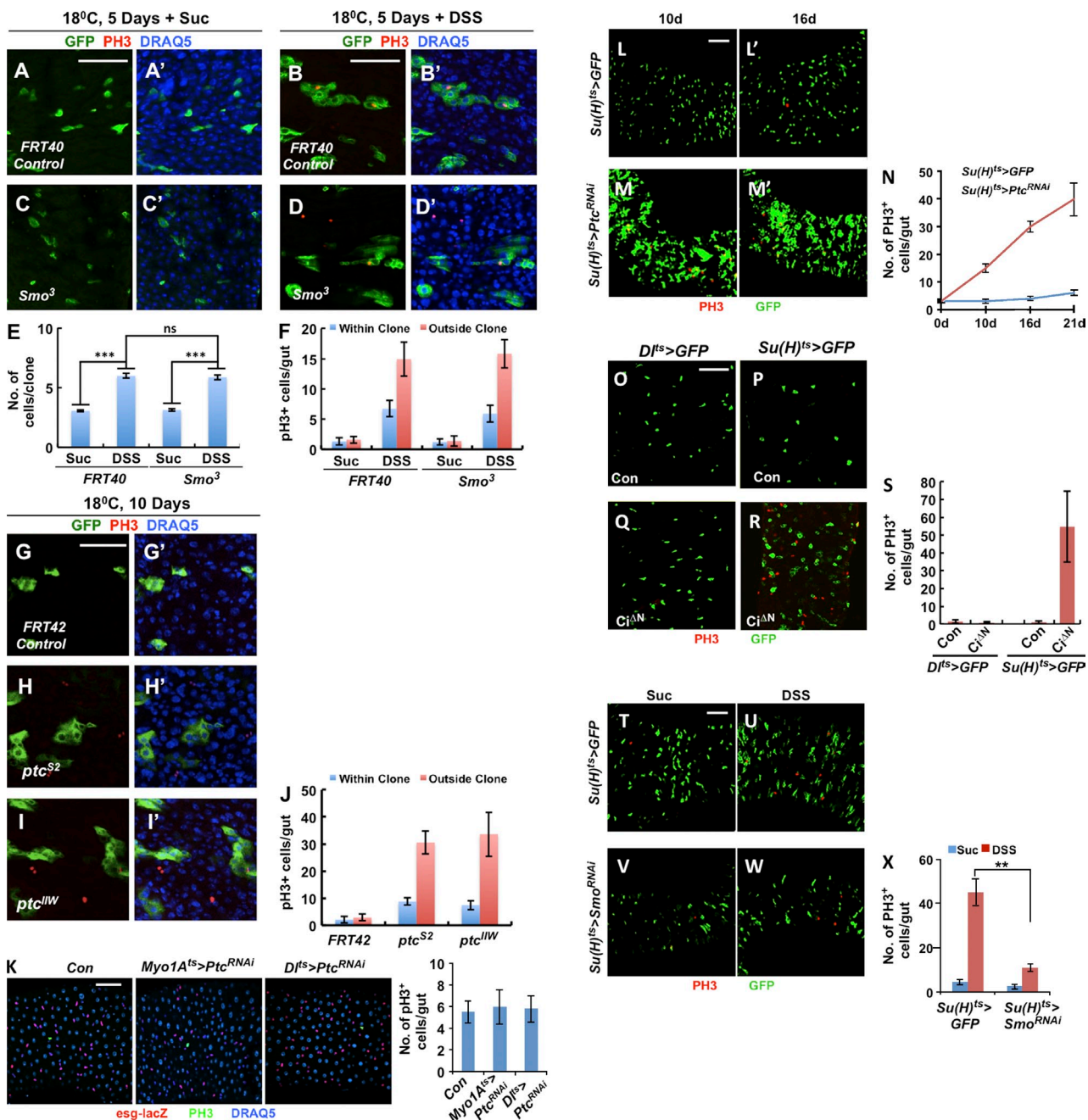
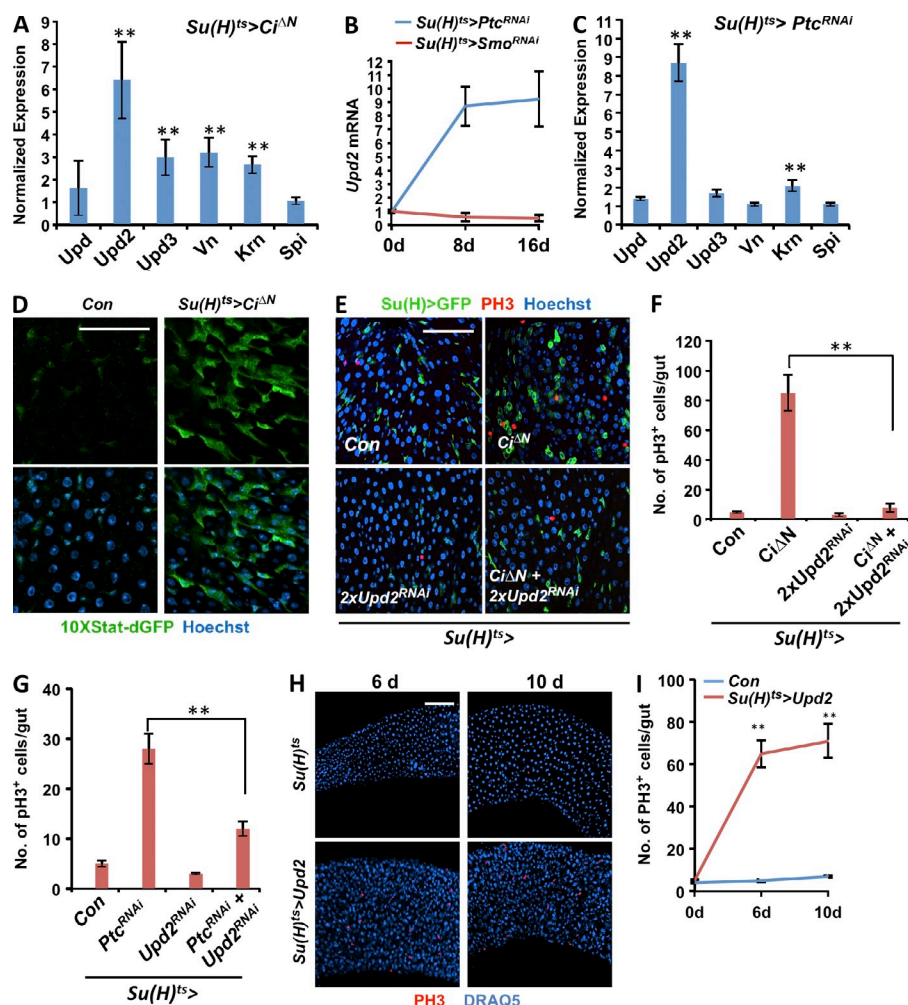


Figure 4. Hh signaling regulates ISC proliferation through the JAK-STAT pathway ligand Upd2. (A and C) mRNA levels of JAK-STAT and EGFR pathway ligands in whole midguts of the flies with indicated genotypes grown at 29°C for 7 (A) or 8 d (C) were measured by RT-qPCR. Numbers indicate fold change over control guts. Three independent experiments were performed, and error bars are standard deviations. **, $P < 0.01$. (B) Relative levels of Upd2 mRNA in midguts expressing $Su(H)^{ts}>Ptc^{RNAi}$ or $Su(H)^{ts}>Smo^{RNAi}$ at the indicated time points. Numbers indicate fold change over control guts from three independent experiments. Error bars are standard deviations. (D) The expression of $10XStat-dGFP$ was elevated in $Su(H)^{ts}>Ci^{\Delta N}$ adult midguts. (E) Midguts expressing $Su(H)^{ts}>GFP$, $Su(H)^{ts}>GFP + Ci^{\Delta N}$, $Su(H)^{ts}>GFP$ plus two copies of $UAS-Upd2^{RNAi}$, or $Su(H)^{ts}>GFP + Ci^{\Delta N} + Upd2^{RNAi}$ (two copies) for 8 d were dissected out and immunostained for GFP (green), PH3 (red), and Hoechst (blue). (F and G) Quantification of PH3⁺ cells in adult midguts of the indicated genotypes grown at 29°C for 8 (F) or 12 d (H). Of note, only one copy of $UAS-Upd2^{RNAi}$ was coexpressed with $UAS-Ptc^{RNAi}$ (G). Three independent experiments were performed and 20 guts were examined for each sample. Error bars are standard deviations. **, $P < 0.01$. (I) Adult flies expressing $Su(H)^{ts}$ (Con) or $Su(H)^{ts}>Upd2$ for the indicated time at 29°C were dissected out and immunostained for PH3 (red) and DRAQ5 (blue). (J) Quantification of PH3⁺ cells in midguts expressing $Su(H)^{ts}$ (Con) or $Su(H)^{ts}>Upd2$ for the indicated time. Three independent experiments were performed and 20 guts were examined for each sample. Error bars are standard deviations. **, $P < 0.01$. Bars, 50 μm .



ligands, including Vn, Krn, and Spi, exhibited no significant change or modest up-regulation in response to Hh pathway activation (Fig. 4, A–C). Indeed, we found that the JAK-STAT pathway reporter gene $10XStat-dGFP$ was activated upon overexpression of the active form of Ci ($Su(H)^{ts}>Ci^{\Delta N}$; Fig. 4 D). In addition, the basal expression of Upd2 was reduced in midguts expressing $Su(H)^{ts}>Smo^{RNAi}$ (Fig. 4 B).

The observation that Hh pathway activation up-regulated the production of Upd2 suggests that Hh signaling regulated ISC proliferation noncell autonomously through the JAK-STAT pathway. In support of this notion, we found that knockdown of Upd2 in EBs suppressed ISC overproliferation caused by $Su(H)^{ts}>Ci^{\Delta N}$ or $Su(H)^{ts}>Ptc^{RNAi}$ (Fig. 4, E–G). In contrast, ectopic expression of Upd2 in EBs ($Su(H)^{ts}>Upd2$) caused overproliferation of ISCs (Fig. 4, H and I). Collectively, these results suggest that elevated Hh signaling in EBs increases the production of Upd2, which in turn activates the JAK-STAT pathway to fuel ISC proliferation.

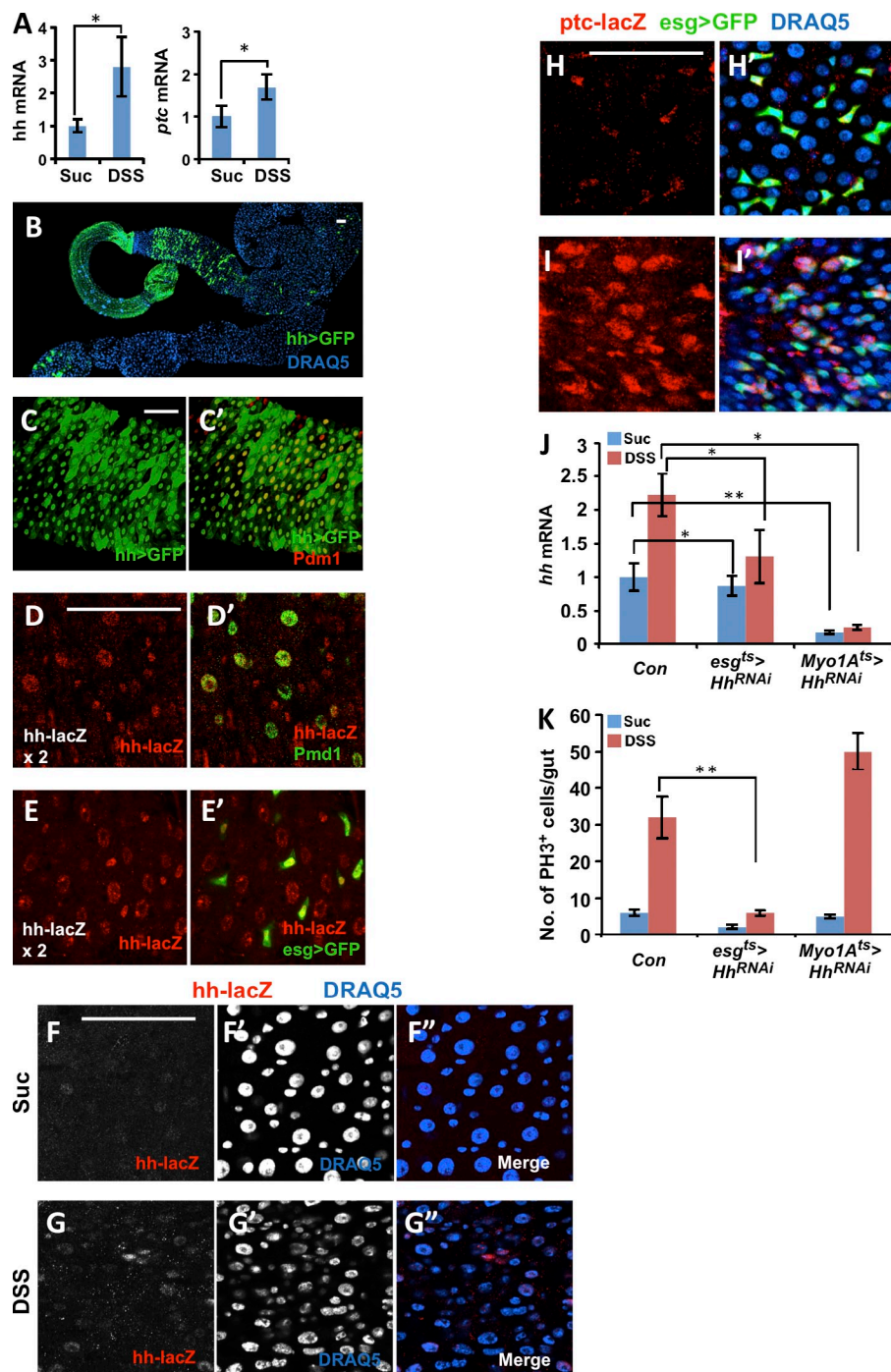
Hh signaling is up-regulated by DSS

The observation that Hh signaling is not essential for basal ISC proliferation but is required for damage-induced ISC proliferation prompted us to examine whether Hh pathway activity is up-regulated in response to injury. Using RT-qPCR,

we found that the expression of the Hh pathway target gene *ptc* as well as *hh* itself was up-regulated in guts treated with DSS; however, expression of *hh* was not induced by bleomycin treatment (Fig. 5 A and Fig. S2).

To determine which cells express the Hh ligand, we examined the expression of *hh-lacZ* as well as GFP driven by *hh-Gal4* (*hh>GFP*) in midguts. The expression of both *hh-lacZ* and *hh>GFP* was detected in Pdm1 ECs with strong expression in the posterior region of midguts as well as in hindguts (Fig. 5, B–D'; and Fig. S2). In addition, *hh-lacZ* was also detected in *esg>GFP*⁺ cells including both EBs and ISCs (Fig. 5, E and E'; and Fig. S3, A–A'), suggesting that Hh is produced by both precursor and mature cells of midgut epithelia. Consistent with the RT-qPCR results, we found that the expression of *hh-lacZ* and *hh>GFP* was up-regulated after DSS treatment, whereas the expression of *hh>GFP* was not stimulated in midguts treated with bleomycin (Fig. 5, F and G; and Fig. S2). Because DSS and bleomycin cause distinct tissue damages in midguts (Amcheslavsky et al., 2009), these results suggest that Hh signaling is differentially regulated in response to different tissue damages.

To determine which cells respond to Hh, we examined midguts carrying the Hh pathway reporter gene *ptc-lacZ*. *ptc-lacZ* was detected in precursor cells but not in ECs under normal



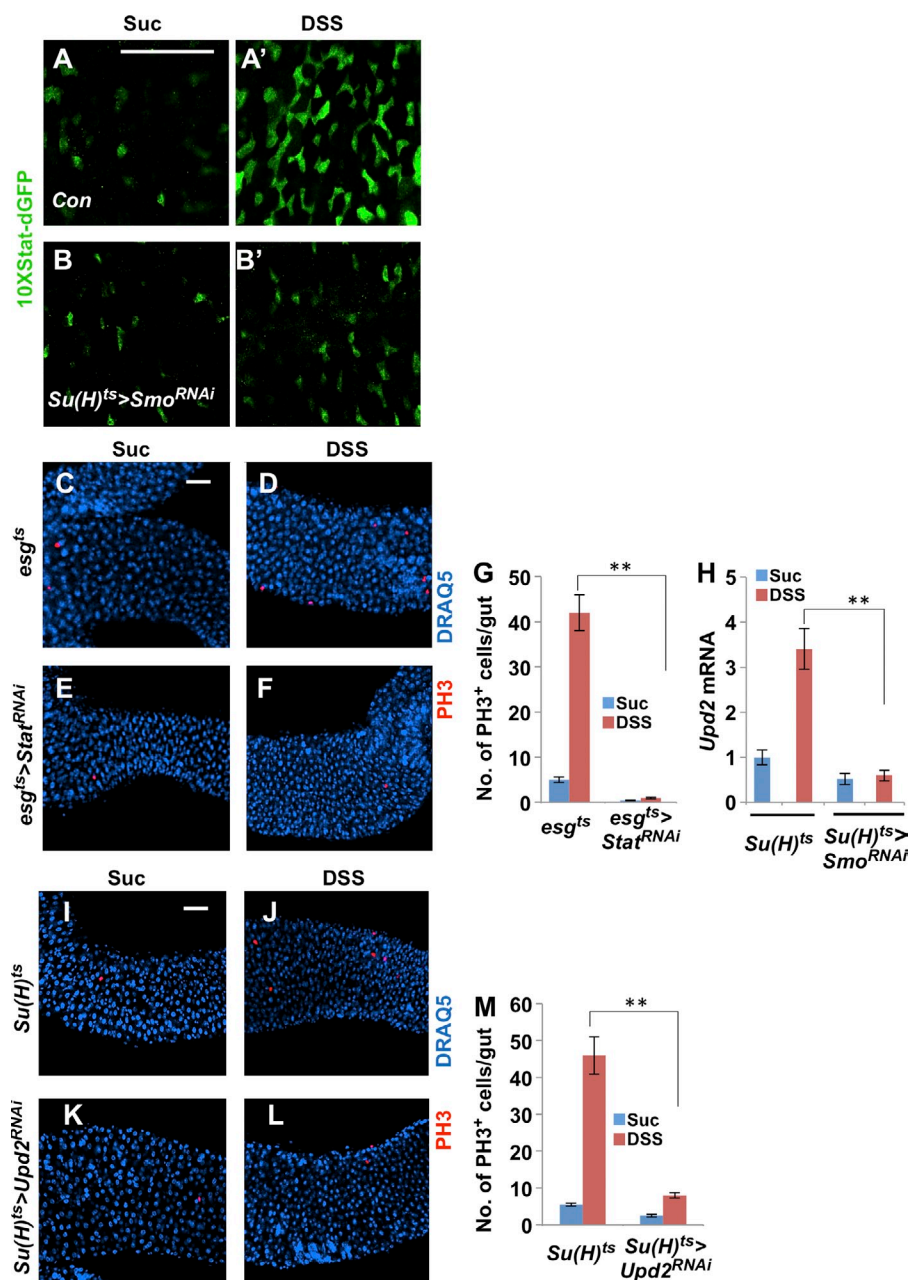
tissue homeostasis (Fig. 5, H and H'; and Fig. S3, B–B'', C, and C'), and this expression was diminished by inactivation of Smo but stimulated by expression of Ci^{ΔN} (Fig. S3, D–E'), confirming that *ptc-lacZ* expression in precursor cells was regulated by Hh signaling. Importantly, we found that *ptc-lacZ* expression in precursor cells was elevated in response to DSS treatment (Fig. 5, I and I').

Precursor-derived Hh is required for regenerative ISC proliferation

To determine which source of Hh signal is essential for injury-induced ISC proliferation, we knocked down Hh either

in ECs or in precursor cells by expressing *Myo1A^{ts}>Hh^{RNAi}* or *esg^{ts}>Hh^{RNAi}*, respectively. Two independent *UAS-Hh^{RNAi}* lines (Bloomington Drosophila Stock Center [BL] 25794 and Vienna Drosophila Resource Center [VDRC] 43255) were used, and similar results were obtained. RT-qPCR confirmed that *Myo1A^{ts}>Hh^{RNAi}* diminished *hh* mRNA levels in both control and DSS-treated guts, consistent with the findings that *hh>GFP* and *hh-lacZ* were mainly expressed in ECs (Fig. 5 J). In line with the observation that *hh-lacZ* was detected in the precursor cells, *esg^{ts}>Hh^{RNAi}* reduced the expression of *hh* mRNA albeit less dramatically compared with *Myo1A^{ts}>Hh^{RNAi}* (Fig. 5 J). Surprisingly, we found that knockdown of Hh in ECs did not

Figure 6. Hh signaling is required for DSS-stimulated Upd2 expression. (A–B') Expression of *10XStat-dGFP* in adult midguts expressing *Su(H)^{ts}* (Con; A and A') or *Su(H)^{ts}>Smo^{RNAi}* (B and B') and treated with Suc or DSS for 1 d. (C–F) Adult female flies expressing *esg^{ts}* or *esg^{ts}>Stat^{RNAi}* for 8 d at 29°C were treated with Suc or DSS for 1 d before midguts were dissected out and immunostained for PH3 and DRAQ5. (G) Quantification of PH3⁺ cells in midguts of the indicated genotypes treated with Suc or DSS after adult flies were raised for 10 d at 29°C. Three independent experiments were performed and 20 guts were examined for each sample. Error bars are standard deviations. **, $P < 0.01$. (H) Quantification of *Upd2* mRNA levels by RT-qPCR in *Su(H)^{ts}* or *Su(H)^{ts}>Smo^{RNAi}* midguts treated with Suc or DSS. Three independent experiments were performed and error bars are standard deviations. **, $P < 0.01$. (I–L) Adult flies expressing *Su(H)^{ts}* or *Su(H)^{ts}>Upd2^{RNAi}* for 10 d at 29°C were treated with Suc or DSS for 1 d before midguts were dissected out and immunostained for PH3 and DRAQ5. (M) Quantification of PH3⁺ cells in midguts of the indicated genotypes treated with Suc or DSS. Three independent experiments were performed and 20 guts were examined for each sample. Error bars are standard deviations. **, $P < 0.01$. Bars, 50 μ m.



block DSS-induced ISC proliferation whereas knockdown of Hh in precursor cells diminished DSS-stimulated ISC proliferation (Fig. 5 K). These results suggest that precursor cell-derived Hh ligands are essential for DSS-induced ISC proliferation.

DSS induces Upd2 production through the Hh pathway

If DSS-mediated tissue damage stimulates ISC proliferation through the Hh signaling pathway, one would predict that feeding adult flies with DSS should induce Upd2 production and activate the JAK–STAT pathway. Indeed, we found that the JAK–STAT pathway reporter gene *10XStat-dGFP* was activated in response to DSS treatment and that DSS-induced up-regulation of *10XStat-dGFP* was blocked by inactivation of Hh signaling in EBs (*Su(H)^{ts}>Smo^{RNAi}*; Fig. 6, A–B'). Furthermore,

knockdown of STAT in precursor cells (*esg^{ts}>Stat^{RNAi}*) blocked DSS-induced ISC proliferation (Fig. 6, C–G), suggesting that DSS-mediated tissue damage stimulates ISC through the JAK–STAT pathway.

Using RT-qPCR, we found that *Upd2* expression was up-regulated in midguts treated with DSS (Fig. 6 H, left columns). Importantly, DSS-induced *Upd2* up-regulation was blocked by Smo RNAi in EBs (*Su(H)^{ts}>Smo^{RNAi}*; Fig. 6 H, right columns), suggesting that DSS induces *Upd2* expression through Hh signaling. Finally, we found that knockdown of Upd2 in EBs (*Su(H)^{ts}>Upd2^{RNAi}*) significantly inhibited DSS-induced ISC proliferation (Fig. 6, I–M). Collectively, these results suggest that injury-induced Hh pathway activation and Upd2 production is required for regenerative ISC proliferation in response to DSS-mediated tissue damage.

DSS up-regulates Hh through the JNK pathway

Many types of cellular stresses can activate the JNK pathway (Weston and Davis, 2007). Indeed, we found that midguts fed with DSS activated the JNK pathway reporter *puc-lacZ* in *Su(H)>GFP*⁺ EBs as well as adjacent ECs, whereas mock treatment barely activated *puc-lacZ* in these cells (Fig. 7, A–B'). To determine whether JNK pathway activation is required for DSS-induced Hh pathway activation, we blocked the JNK pathway by expressing a dominant-negative Basket, *Bsk*^{DN}, in EBs (*Su(H)^{ts}>Bsk^{DN}*). We found that *Su(H)^{ts}>Bsk^{DN}* blocked DSS-induced Hh up-regulation and ISC proliferation (Fig. 7, C and D).

To determine whether JNK signaling can induce Hh pathway activation in midguts, we activated the JNK pathway by knocking down the inhibitory component Puckered (*Puc*) in EBs (*Su(H)^{ts}>Puc^{RNAi}*). We found that *Su(H)^{ts}>Puc^{RNAi}* or *esg^{ts}>Puc^{RNAi}* up-regulated the expression of both *hh* and *ptc*, as determined by RT-qPCR and *lacZ* reporter gene expression (Fig. 7, E–I'). In addition, we found that Hh RNAi greatly suppressed ISC proliferation induced by *Puc* RNAi in precursor cells (Fig. 7, J–N). These results suggest that JNK signaling in precursor cells stimulates Hh production, which contributes to JNK pathway-induced ISC proliferation. Hence JNK signaling is both necessary and sufficient to induce Hh pathway activation.

Discussion

Many adult organs undergo stem cell-based repair/regeneration but the underlying regulatory mechanisms are still not well understood. Here we use *Drosophila* adult midgut as a model to investigate the role of Hh signaling in adult tissue homeostasis and regeneration. We found that basal Hh pathway activity in ISC lineage is dispensable for homeostatic ISC proliferation but elevated Hh signaling is essential for regenerative proliferation of ISCs. We demonstrated that Hh signaling promotes ISC proliferation noncell autonomously through the JAK–STAT pathway ligand *Upd2* (Fig. 7 O).

In addition to their role as morphogen to control cell patterning, the secreted Hh glycoproteins have also been implicated as mitogen to regulate cell proliferation in embryonic development, adult tissue homeostasis, and many types of cancers

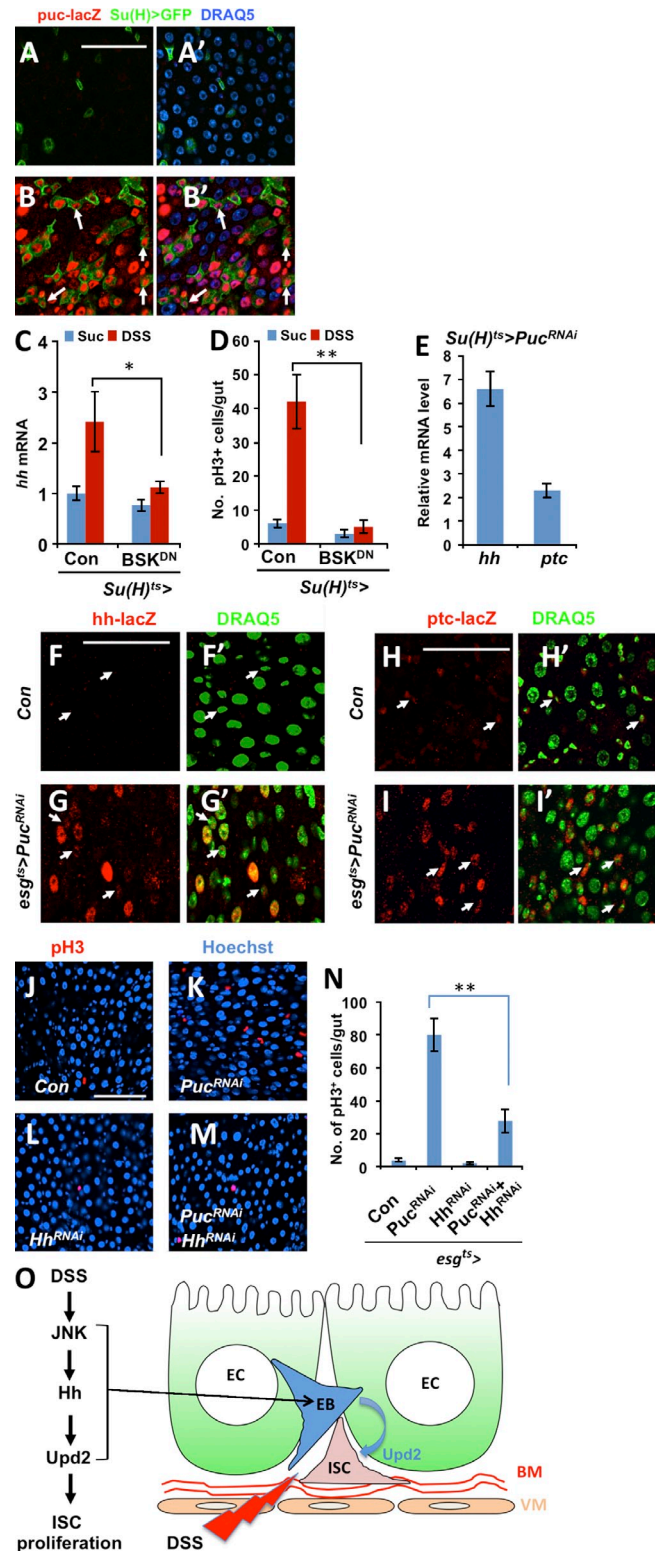


Figure 7. DSS up-regulates Hh signaling through the JNK pathway. (A–B') Expression of a JNK pathway reporter, *puc-lacZ*, in mock (Suc; A and A') or DSS-treated (B and B') midguts for 1 d. *puc-lacZ* expression was barely detectable in mock-treated guts but was elevated in *Su(H)>GFP*-positive cells in DSS-treated guts. Arrows indicate *Su(H)>GFP*⁺ cells with small nuclei. (C) Quantification of relative *hh* mRNA levels by RT-qPCR in control or *Su(H)^{ts}>Bsk^{DN}* midguts treated with Suc or DSS for 1 d after adult flies were raised at 29°C for 10 d. Three independent experiments were performed and error bars are standard deviations. *, *P* < 0.05. (D) Quantification of PH3⁺ cells in control or *Su(H)^{ts}>Bsk^{DN}* midguts treated with Suc or DSS for 1 d after adult flies were raised for 10 d at 29°C. Three independent experiments were performed and 20 guts were examined for each sample. Error bars are standard deviations. **, *P* < 0.01. (E) Quantification of *hh* and *ptc* mRNA levels by RT-qPCR in control and *Su(H)^{ts}>Puc^{RNAi}* guts grown at 29°C for 6 d. Three independent experiments were performed and error bars are standard deviations. Numbers indicate fold change over control guts. (F–I') Expression of *hh-lacZ* (F–G', red) or *ptc-lacZ* (H–I', red) in control (F, F', H, and H') or *esg^{ts}>Puc^{RNAi}*

guts grown at 29°C for 5 d. Arrows indicate elevated *hh-lacZ* (F–G') and *ptc-lacZ* (H–I') in precursor cells. (J–M) Adult midguts expressing *esg^{ts}* (Con; J), *esg^{ts}>Puc^{RNAi}* (K), *esg^{ts}>Hh^{RNAi}* (L), or *esg^{ts}>Puc^{RNAi} + Hh^{RNAi}* (M) for 7 d at 29°C were dissected out and immunostained for PH3 and Hoechst. (N) Quantification of PH3⁺ cells in adult midguts of the indicated genotypes. Three independent experiments were performed and 20 guts were examined for each sample. Error bars are standard deviations. **, *P* < 0.01. (O) A JNK–Hh–JAK–STAT signaling axis mediates DSS-stimulated ISC proliferation in adult midgut regeneration. BM, basement membrane; VM, visceral muscles. See text for details. Bars, 50 μ m.

(Jiang and Hui, 2008). In mammals, early studies revealed that Hh signaling was essential for normal intestinal development and that Indian Hh promoted colonic epithelial cell differentiation by antagonizing Wnt signaling in adult colon (Ramalho-Santos et al., 2000; van den Brink et al., 2004; Madison et al., 2005). However, more recent studies revealed that Hh signaling was essential for colon cancer development and stem cell expansion in APC mutant backgrounds (Arimura et al., 2009; Varnat et al., 2009, 2010). Consistent with a mitogenic role of Hh signaling in gastrointestinal cancers, Hh ligand production and signaling were elevated in these tumors (Berman et al., 2003); however, it remained controversial regarding whether Hh signaling acted in a cell-autonomous (autocrine) or nonautonomous (paracrine) fashion to promote tumor growth (Berman et al., 2003; Yauch et al., 2008; Singh et al., 2011). Hh signaling has also been implicated in tissue regeneration and repair in organs including lung, prostate, pancreas, liver, bladder, skin, and bone (Beachy et al., 2004; Fendrich et al., 2008; Ochoa et al., 2010; Shin et al., 2011; Bielefeld et al., 2013; Peng et al., 2013). However, with a few exceptions (Shin et al., 2011; Hsu et al., 2014), the precise locations where Hh signaling acts and/or the downstream effectors that mediate the biological function of Hh signaling have remained largely unknown.

Taking advantage of the sophisticated toolkit available to manipulate gene function in specific cellular compartments of *Drosophila* adult midgut, we provided several lines of evidence that Hh signaling acts in EBs rather than in ISCs to regulate ISC proliferation in response to injury. *smo* mutant ISC lineage clones grew normally in the absence or presence of injury, suggesting that Hh pathway activity is not required in the stem cells for midgut homeostasis and regeneration. Inactivation of Hh signaling in EBs blocked injury-induced ISC proliferation. Activation of Hh signaling either by Ptc RNAi or overexpression of an active form of Ci in EBs but not in ISCs stimulated ISC proliferation. *ptc* mutant clones induced ectopic proliferation of neighboring wild-type ISCs. Collectively, these results demonstrated that Hh signaling acts noncell autonomously to drive ISC proliferation. Of note, a recent study suggested that Hh signaling acted in stem cells to directly regulate their proliferation (Li et al., 2014); however, this notion was solely based on manipulation of Hh pathway activity in *esg*⁺ cells that include both ISCs and EBs. In contrast, we demonstrated that Hh signaling acted in EBs but not in ISCs to indirectly regulate ISC proliferation. Li et al. (2014) also found that *smo* mutant clones exhibited reduced clone size compared with age-matched control clones. In contrast, we found that *smo* null clones grew at a rate similar to that of control clones either under normal homeostasis or in response to DSS treatment (Fig. 3). It is possible that differences in the *smo* alleles and experimental conditions used in these two studies caused the discrepancy. Nonetheless, we noticed that the growth deficit of *smo* mutant clones observed by Li et al. (2014) is very mild.

In search for Hh-regulated secreted proteins that mediate the effect of Hh signaling on ISC proliferation, we found that Hh pathway activation dramatically increased the expression of the JAK–STAT pathway ligand Upd2 as well as the pathway reporter gene *10XStat-dGFP*. Importantly, depletion of Upd2 diminished ISC proliferation induced by Hh pathway activation. Further

study is required to determine whether Upd2 is a direct target of Hh signaling in midgut regeneration. We noticed that other JAK–STAT pathway ligands such as Upd3 and EGFR ligands including Vn and Krn were slightly up-regulated upon Hh pathway activation, which may also contribute to ISC proliferation stimulated by Hh signaling. Interestingly, a recent study showed that Hh pathway activation by expression of an oncogenic Smo (SmoM2) in skin up-regulated IL-11 and IL-11Ra expression and STAT3 phosphorylation and that IL-11Ra/STAT3 signaling mediated SmoM2-driven carcinogenesis (Gu et al., 2012). Hence, the Hh–JAK–STAT signaling axis we uncovered here is evolutionarily conserved and likely to be used by many other systems.

Midgut injury results in excessive production of mitogens including the JAK–STAT and EGFR pathway ligands to stimulate regenerative ISC proliferation, but the mechanism linking changes in mitogen production to many types of injuries have remained largely unexplored. The regulation could be complex and might vary depending on the nature of injury. For example, infection of adult flies with *Pseudomonas entomophila* activated JNK pathway and up-regulated Upd3 production in ECs, and JNK pathway activation in ECs sufficed to increase Upd3 production; however, blocking JNK pathway in ECs did not block *P. entomophila*–induced Upd3 production and ISC proliferation, suggesting that *P. entomophila* infection up-regulated Upd3 production through multiple pathways (Jiang et al., 2009). Inactivation of Hpo pathway effector Yki in precursor cells inhibited DSS-induced Myc activation and ISC proliferation but had little if any effect on bleomycin-induced Myc activation and ISC proliferation (Ren et al., 2010, 2013), suggesting that DSS and bleomycin elicited distinct regenerative responses, which is in line with the observation that DSS and bleomycin caused different types of damages to the midguts (Amcheslavsky et al., 2009). Interestingly, we found that Hh signaling was elevated by DSS but not by bleomycin treatment. Furthermore, inhibition of Hh signaling in EBs blocked DSS-stimulated Upd2 production, JAK–STAT pathway activation, and ISC proliferation. Although bleomycin treatment did not increase Hh production, inhibition of Hh signaling also reduced bleomycin-stimulated ISC proliferation, suggesting that basal Hh signaling is required for the optimal ISC proliferation in response to bleomycin-mediated tissue damage. Interestingly, Hh was also up-regulated in adult midguts in response to bacterial infection (Buchon et al., 2009b), suggesting that Hh signaling may play a broad role in regulating regenerative proliferation of ISCs in response to various stimuli.

We found that DSS induced JNK pathway activation in EBs and that JNK pathway activity in these cells was necessary for DSS-induced Hh pathway activation. Furthermore, we showed that ectopic JNK signaling activity in precursor cells sufficed to induce Hh pathway activation and that Hh RNAi attenuated ISC proliferation induced by JNK activation, suggesting that Hh signaling mediates ISC proliferation in response to JNK-mediated stress in precursor cells. Intriguingly, Li et al. (2014) showed that *puc-lacZ* was broadly up-regulated when Ptc was knocked down in precursor cells although it is not clear how ectopic Hh signaling leads to JNK pathway activation. It is possible that Hh-driven ISC overproliferation could induce cellular stress, which indirectly activated the JNK pathway.

Indeed, we found that overexpression of Upd2 in EBs not only stimulated ISC proliferation but also broadly activated *pucc-lacZ* expression (unpublished data). Therefore, it is possible that a positive feedback loop may exist between JNK and mitogenic signals, which could fuel more rapid ISC proliferation in response to injury. Further study is needed to explore the complex relationships between the JNK and various mitogenic pathways in the regulation of ISC proliferation.

Materials and methods

Drosophila genetics and transgenes

The following fly strains were used: *smo*³ contains a stop codon at aa 366 (W366Z) and behaves like a null allele (Chen and Struhl, 1998); *ptc*^{l^W} is a genetic null allele (Nakano et al., 1989); *ptc*^{S2} contains a D584N mutation in the sterol-sensing domain of Ptc (Martin et al., 2001); *cos2*² is a genetic null allele (Sisson et al., 1997); *UAS-Ptc*^{RNAi} (BL 28795); *UAS-Smo*^{RNAi} (BL 27037); *UAS-Cr*^{RNAi} (VDR 51479); *UAS-Hh*^{RNAi} (VDR 43255 and BL 25794); *UAS-Upd2*^{RNAi} (VDR 14664 and BL 33949); *UAS-Star*^{RNAi} (VDR 43866); *UAS-Puc*^{RNAi} (VDR 3018); *UAS-Dicer2* on the X chromosome (BL 24648); *UAS-Dicer2* on the second chromosome (BL 24650); *UAS-Cr^{ΔN}* expresses a Ci variant lacking the N-terminal 439 residues (Wang et al., 2000); *UAS-BSK*^{DN} expresses a dominant-negative form of BSK (BL 6409); *Su(H)-Gal4* contains three copies of the GRH binding elements and two copies of Su(H) binding sites fused to *GAL4* coding sequence; *Delta*(*DI*)-*Gal4* has a *Gal4* coding sequence inserted in the *DI* locus (Zeng et al., 2010); *hh-Gal4* (a *Gal4* enhancer trap insertion in the *hh* locus); *esg-Gal4* (a *GAL4* enhancer trap insertion in the *esg* locus); *Myo1A-Gal4* (a *Gal4* enhancer trap insertion in the *Myosin 1A* locus); *How-Gal4* (*how*^{24B}) is a *Gal4* enhancer trap insertion in the *how* locus (BL 1768); *tub-Gal80*^S expresses a temperature-sensitive *Gal80* under the control of tubulin promoter (McGuire et al., 2004); *ptc-lacZ* (a *ptc* enhancer element fused to *lacZ*); *hh-lacZ* (*hh*^{P30}, a *lacZ* enhancer trap at the *hh* locus); and *10XStatdGFP* (a JAK-STAT pathway reporter gene that contains 10 copies of STAT binding sites fused to a *GFP* coding sequence; Bach et al., 2007). Flies were maintained on standard media and were changed into vials containing fresh food every 2 d. Of note, for cell type-specific inactivation of Ptc, Smo, or Hh, two copies of the corresponding *UAS* transgenic RNAi lines were expressed to achieve optimal knockdown of the targeted genes. In addition, *UAS-Dicer2* was coexpressed to further enhance the knockdown efficiency. See Genotypes for figures and supplemental figures section for the complete genotypes of individual experiments.

Clone induction and transgene activation by Gal4 in conjunction with Gal80^S

Mutant clones for *smo*³*FRT40A*, *FRT42Dptc*^{S2} or *l^W*, or *FRT42Dcos2*² were generated using the MARCM system (Lee and Luo, 2001) with the corresponding stocks: *hs-flp UAS-GFP*; *tub-Gal80 FRT40A*; *tub-Gal4/TM6B* and *hs-flp UAS-GFP*; *FRT42D tub-Gal80*; *tub-Gal4/TM6B*. *FRT40A* and *FRT42D* (FlyBase) were used as wild-type control. To induce MARCM clones, fly stocks were crossed and cultured at 18°C, and 3- to 5-d-old F1 adult flies with the appropriate genotypes were subjected to heat shock in empty vials for 1 h in a 37°C water bath. After clone induction, flies were transferred to new cornmeal food every 2 d and raised at 18°C for 10 or 20 d before dissection. For experiments involving *Gal4/Gal80*^S, crosses were set up and cultured at 18°C to restrict *Gal4* activity. 2- to 3-d-old F1 adult flies were then shifted to 29°C to inactivate *Gal80*^S, allowing *Gal4* to activate *UAS* transgenes. The guts were dissected out and analyzed by confocal microscopy.

Feeding experiments

In general, 2- to 3-d-old F1 adult flies were shifted to 29°C to inactivate *Gal80*^S for 8 d or longer to allow RNAi to take full effect. The flies were then used for feeding experiments. Flies were cultured in an empty vial containing a piece of 2.5 × 3.75-cm chromatography paper (Thermo Fisher Scientific) wet with 5% sucrose (Suc) solution as feeding medium. Flies were fed with 5% of DSS (MP Biomedicals) or 25 μg/ml bleomycin (Sigma-Aldrich) dissolved in 5% Suc (mock treatment) for 1 d at 29°C.

Immunostaining and microscopy

Female flies were used for gut immunostaining in all experiments. The entire gastrointestinal tracts were dissected out and fixed in PBS plus 8% EM grade paraformaldehyde (Polysciences) for 2 h. Samples were washed and

incubated with primary and secondary antibodies in a solution containing PBS, 0.5% BSA, and 0.1% Triton X-100. The following primary antibodies were used: mouse anti-Pros (Developmental Studies Hybridoma Bank), 1:100; rabbit anti-LacZ (MP Biomedicals), 1:1,000; rabbit and mouse anti-PH3 (EMD Millipore), 1:1,000; goat anti-GFP (Abcam), 1:1000; rabbit anti-Pdm1 (aa 95–256; gift from X. Yang, Institute of Molecular and Cell Biology, Singapore, Singapore); DRAQ5 (Cell Signaling Technology), 1:5,000; Hoechst (Life technologies), 1:500. Alexa Fluor-conjugated secondary antibodies were used at 1:400 (Jackson ImmunoResearch Laboratories, Inc., and Invitrogen). Guts were mounted in 70% glycerol and imaged with a confocal microscope (LSM 510 inverted; Carl Zeiss) using 10x, 20x, and 40x oil objectives (imaging medium: Immersol 518F; Carl Zeiss). The imaging temperature was room temperature. The acquisition and processing software was LSM Image Browser (Carl Zeiss) and image processing was done in Photoshop CC (Adobe).

RT-qPCR

Total RNA was extracted from 15 female guts using RNeasy Plus mini kit (QIAGEN), and cDNA was synthesized using the iScript cDNA synthesis kit (Bio-Rad Laboratories). RT-qPCR was performed using iQ SYBR Green System (Bio-Rad Laboratories). RT-qPCR was performed in triplicate on each of three independent biological replicates. Primer sequences used are: 5'-GGTACCAAGTCTTAGCTTC-3' and 5'-CAGCCAAGGACGAGTTATCA-3' (for *upd2*), 5'-CGGAATCAGCGGTCTGTATAC-3' and 5'-ATTACAGTGGGTTCAGGCAG-3' (for *ptc*), 5'-GGATTCGATTGGGTCTCTAC-3' and 5'-GGGAACTGATCGACGAATCT-3' (for *hh*), 5'-CCACGTAAGTTTGCATGTTG-3' and 5'-CTAAACAGTAGCCAGGACTC-3' (for *upd*), 5'-GAG-CAACCAAGACTCTGGACA-3' and 5'-CCAGTGCAACTTGATGTTG-3' (for *upd3*), 5'-TCACACATTAGTGGTGAAG-3' and 5'-TTGTGATGCTTGAATTGGTAA-3' (for *vn*), 5'-CGTGTGTTGGCAACAACAAGT-3' and 5'-TGTGGCAATGCAGTTTAAGG-3' (for *krrn*), and 5'-CGCCCAAGAATGAAAGAGAG-3' and 5'-AGGTATGCTGCTGTGGGAAC-3' (for *sp*). Rpl11 was used as a normalization control. Relative quantification of mRNA levels was calculated using the comparative C_T method.

Genotypes for figures and supplemental figures

Figure 1. (A and A') *yw*; *UAS-GFP hsf**l**p*; *FRT42 tub-Gal80/FRT42*; *tub-Gal4/+*. (B and B') *yw* *UAS-GFP hsf**l**p*; *FRT42 tub-Gal80/FRT42 ptc*^{l^W}; *tub-Gal4/+*. (C and C') *yw* *UAS-GFP hsf**l**p*; *FRT42 tub-Gal80/FRT42 ptc*^{S2}; *tub-Gal4/+*. (D and D') *yw* *UAS-GFP hsf**l**p*; *FRT42 tub-Gal80/FRT42 cos2*²; *tub-Gal4/+*. (F, F', I, and I') *yw* *UAS-GFP hsf**l**p*; *tub-Gal80 FRT40/FRT40*; *tub-Gal4/+*. (G, G', J, and J') *yw* *UAS-GFP hsf**l**p*; *tub-Gal80 FRT40/smo*³ *FRT40*; *tub-Gal4/+*.

Figure 2. (A–C) *w*; *esg-Gal4 tub-Gal80*^S/+; *UAS-GFP/+*. (D–F) *w*; *esg-Gal4 tub-Gal80*^S/+; *UAS-GFP/UAS-Smo*^{RNAi}. (G–I) *w*; *esg-Gal4 tub-Gal80*^S/+; *UAS-GFP/UAS-Cr*^{RNAi}. (K and L) *Su(H)-lacZ*; *esg-Gal4 tub-Gal80*^S *UAS-GFP/+*; *UAS-flp, act>CD2>gal4/+*. (M and N) *w*; *esg-Gal4 tub-Gal80*^S *UAS-GFP/+*; *UAS-flp, act>CD2>gal4/+*. (O and P) *Su(H)-lacZ*; *esg-Gal4 tub-Gal80*^S *UAS-GFP/+*; *UAS-flp, act>CD2>gal4/UAS-Smo*^{RNAi}. (Q and R) *w*; *esg-Gal4 tub-Gal80*^S *UAS-GFP/+*; *UAS-flp, act>CD2>gal4/UAS-Smo*^{RNAi}.

Figure 3. (A–B') *yw* *UAS-GFP hsf**l**p*; *tub-Gal80 FRT40/FRT40*; *tub-Gal4/+*. (C–D') *yw* *UAS-GFP hsf**l**p*; *tub-Gal80 FRT40/smo*³ *FRT40*; *tub-Gal4/+*. (G and G') *yw* *UAS-GFP hsf**l**p*; *FRT42 tub-Gal80/FRT42*; *tub-Gal4/+*. (H and H') *yw* *UAS-GFP hsf**l**p*; *FRT42 tub-Gal80/FRT42 ptc*^{S2}; *tub-Gal4/+*. (I and I') *yw* *UAS-GFP hsf**l**p*; *FRT42 tub-Gal80/FRT42 ptc*^{l^W}; *tub-Gal4/+*. (K) *yw* (Con), *yw*; *myo1A-Gal4 tub-Gal80*^S/+; *UAS-Dicer2*; *UAS-Ptc*^{RNAi}/+; *UAS-Ptc*^{RNAi}, and *yw*; *tub-Gal80*^S/+; *UAS-Dicer2*; *DI-Gal4 UAS-Ptc*^{RNAi}/+; *UAS-Ptc*^{RNAi}. (L, L', P, T, and U) *w*; *Su(H)-Gal4 tub-Gal80*^S *UAS-GFP/UAS-Dicer2*; +/+; (M and M') *w*; *Su(H)-Gal4 tub-Gal80*^S *UAS-GFP/UAS-Dicer2*; *UAS-Ptc*^{RNAi}/+; *UAS-Ptc*^{RNAi}. (R) *w*; *Su(H)-Gal4 tub-Gal80*^S *UAS-GFP/+*; *UAS-Cr*^{ΔN}/+. (O) *w*; *tub-Gal80*^S *UAS-GFP/+*; *DI-Gal4/+*. (Q) *w*; *tub-Gal80*^S *UAS-GFP/+*; *DI-Gal4/UAS-Cr*^{ΔN}. (V and W) *w*; *Su(H)-Gal4 tub-Gal80*^S *UAS-GFP/UAS-Dicer2*; *UAS-Smo*^{RNAi}/+; *UAS-Smo*^{RNAi}.

Figure 4. (A) *w*; *Su(H)-Gal4 tub-Gal80*^S *UAS-GFP/+*; +/+ and *w*; *Su(H)-Gal4 tub-Gal80*^S *UAS-GFP/+*; *UAS-Cr*^{ΔN}/+. (B) *w*; *Su(H)-Gal4 tub-Gal80*^S *UAS-GFP/UAS-Dicer2*; +/+; *w*; *Su(H)-Gal4 tub-Gal80*^S *UAS-GFP/UAS-Dicer2*; *UAS-Ptc*^{RNAi}/+; *UAS-Ptc*^{RNAi} and *w*; *Su(H)-Gal4 tub-Gal80*^S *UAS-GFP/UAS-Dicer2*; *UAS-Smo*^{RNAi}/+; *UAS-Smo*^{RNAi}. (C) *w*; *Su(H)-Gal4 tub-Gal80*^S *UAS-GFP/UAS-Dicer2*; +/+ and *w*; *Su(H)-Gal4 tub-Gal80*^S *UAS-GFP/UAS-Dicer2*; *UAS-Ptc*^{RNAi}/+; *UAS-Ptc*^{RNAi}. (D) *w*; *Su(H)-Gal4 tub-Gal80*^S/+; *10XStatdGFP*; +/+ (Con), and *w*; *Su(H)-Gal4 tub-Gal80*^S/+; *10XStatdGFP*; *UAS-Cr*^{ΔN}/+. (E and F) *w*; *Su(H)-Gal4 tub-Gal80*^S *UAS-GFP/+*; +/+ (Con), *w*; *Su(H)-Gal4 tub-Gal80*^S *UAS-GFP/+*; *UAS-Cr*^{ΔN}/+, *w*; *Su(H)-Gal4 tub-Gal80*^S *UAS-GFP/UAS-Upd2*^{RNAi} (VDR 14664); *UAS-Upd2*^{RNAi} (BL 33949)/+, and *w*; *Su(H)-Gal4 tub-Gal80*^S *UAS-GFP/UAS-Upd2*^{RNAi} (VDR 14664); *UAS-Cr*^{ΔN}/+; *UAS-Upd2*^{RNAi} (BL 33949). (G) *UAS-Dicer2*; *Su(H)-Gal4*

tub-Gal80^{ts} UAS-GFP/+; +/+, *UAS-Dicer2; Su(H)-Gal4 tub-Gal80^{ts} UAS-GFP/+; UAS-Ptc^{RNAi}/UAS-Ptc^{RNAi}, UAS-Dicer2; Su(H)-Gal4 tub-Gal80^{ts} UAS-GFP/UAS-Upd2^{RNAi} (VDR 14664); +/+*, *UAS-Dicer2; Su(H)-Gal4 tub-Gal80^{ts} UAS-GFP/UAS-Upd2^{RNAi}; UAS-Ptc^{RNAi}/UAS-Ptc^{RNAi}*. (H and I) *w; Su(H)-Gal4 tub-Gal80^{ts} UAS-GFP/+; +/+* and *w; Su(H)-Gal4 tub-Gal80^{ts} UAS-GFP/+; UAS-Upd2/+*.

Figure 5. (B–C') *w; +/+; hh-Gal4 UAS-GFP/+*. (D–E') *w; +/+; hh-lacZ/hh-lacZ*, (F–G') *w; +/+; hh-lacZ/+*. (H–I') *w; esg-Gal4 tub-Gal80^{ts} UAS-GFP/+; ptc-lacZ/+*. (J and K) *w; esg-Gal4 tub-Gal80^{ts} UAS-GFP/+; +/+*, *w; esg-Gal4 tub-Gal80^{ts} UAS-GFP/+; UAS-Hh^{RNAi} (BL 25794)/UAS-Hh^{RNAi} (BL 25794)*, and *w; Myo1A-Gal4 tub-Gal80^{ts} UAS-GFP/+; UAS-Hh^{RNAi} (BL 25794)/UAS-Hh^{RNAi} (BL 25794)*.

Figure 6. (A–B') *yw UAS-Dicer2; Su(H)-Gal4/10XStat-dGFP; tub-Gal80^{ts}/+* and *yw UAS-Dicer2; Su(H)-Gal4/10XStat-dGFP; UAS-Smo^{RNAi} tub-Gal80^{ts}/UAS-Smo^{RNAi}*. (C, D, and G) *w; esg-Gal4 tub-Gal80^{ts} UAS-GFP/+; +/+*, (E–G) *w; esg-Gal4 tub-Gal80^{ts} UAS-GFP/UAS-Star^{RNAi}; +/+*. (H) *w; Su(H)-Gal4 tub-Gal80^{ts} UAS-GFP/UAS-Dicer2; +/+* and *w; Su(H)-Gal4 tub-Gal80^{ts} UAS-GFP/UAS-Dicer2; UAS-Smo^{RNAi}/UAS-Smo^{RNAi}*. (I, J, and M) *w; Su(H)-Gal4 tub-Gal80^{ts} UAS-GFP/+; +/+*. (K–M) *w; Su(H)-Gal4 tub-Gal80^{ts} UAS-GFP/UAS-Upd2^{RNAi} (VDR 14664); UAS-Upd2^{RNAi}/+* (BL 33949).

Figure 7. (A–B') *w; Su(H)-Gal4 tub-Gal80^{ts} UAS-GFP/+; Puc-lacZ/+*. (C and D) *w; Su(H)-Gal4 tub-Gal80^{ts} UAS-GFP/+; +/+*, and *UAS-Bsk^{DN}; Su(H)-Gal4 tub-Gal80^{ts} UAS-GFP/+; +/+*. (E) *w; Su(H)-Gal4 tub-Gal80^{ts} UAS-GFP/+; +/+* and *w; Su(H)-Gal4 tub-Gal80^{ts} UAS-GFP/UAS-Puc^{RNAi}; +/+*. (F and F') *w; esgGal4 tub-Gal80^{ts} UAS-GFP/+; hh-lacZ/+*. (G and G') *w; esgGal4 tub-Gal80^{ts} UAS-GFP/UAS-Puc^{RNAi}; hh-lacZ/+*. (H and H') *w; esgGal4 tub-Gal80^{ts} UAS-GFP/+; ptc-lacZ/+*. (I and I') *w; esgGal4 tub-Gal80^{ts} UAS-GFP/UAS-Puc^{RNAi}; ptc-lacZ/+*. (J and N) *w; Su(H)-Gal4 tub-Gal80^{ts} UAS-GFP/+; +/+*. (K and N) *w; Su(H)-Gal4 tub-Gal80^{ts} UAS-GFP/UAS-Puc^{RNAi}; +/+*. (L and N) *w; Su(H)-Gal4 tub-Gal80^{ts} UAS-GFP/+; UAS-Hh^{RNAi} (BL 25794)/UAS-Hh^{RNAi} (BL 25794)*. (M and N) *w; Su(H)-Gal4 tub-Gal80^{ts} UAS-GFP/UAS-Puc^{RNAi}; UAS-Hh^{RNAi} (BL 25794)/UAS-Hh^{RNAi} (BL 25794)*.

Figure S1. (A, A', E, and E') *yw UAS-GFP hslfp; FRT42 tub-Gal80/FRT42; tub-Gal4/+*. (B, B', F, and F') *yw UAS-GFP hslfp; FRT42 tub-Gal80/FRT42 ptc^{S2}; tub-Gal4/+*. (C, C', G, and G') *yw UAS-GFP hslfp; FRT42 tub-Gal80/FRT42 ptc^{low}; tub-Gal4/+*. (D, D', H, and H') *yw UAS-GFP hslfp; FRT42 tub-Gal80/FRT42 cos²; tub-Gal4/+*.

Figure S2. (A–C) *w; UAS-GFP/+; hh-Gal4/+*.

Figure S3. (A–A'') *w; esgGal4 UAS-GFP/+; hh-lacZ/hh-lacZ*. (B–B'') *w; Su(H)Gal4 UAS-GFP/+; ptc-lacZ/+*. (C and C') *w; esgGal4 tub-Gal80^{ts} UAS-GFP/+; ptc-lacZ/+*. (D and D') *w; esgGal4 tub-Gal80^{ts} UAS-GFP/+; ptc-lacZ/UAS-Smo^{RNAi}*. (E and E') *w; esgGal4 tub-Gal80^{ts} UAS-GFP/+; ptc-lacZ/UAS-C¹N*.

Online supplemental material

Fig. S1 shows that ectopic Hh pathway activation does not perturb ISC lineage differentiation. Fig. S2 shows that DSS but not bleomycin treatment increased Hh expression. Fig. S3 shows that both Hh-lacZ and Ptc-lacZ are expressed in EBs and ISCs. Online supplemental material is available at <http://www.jcb.org/cgi/content/full/jcb.201409025/DC1>. Additional data are available in the JCB DataViewer at <http://dx.doi.org/10.1083/jcb.201409025.dv>.

We thank Drs. Tony Ip, Steve Hou, and Huaqi Jiang, Vienna Drosophila Resource Center and Bloomington Drosophila Stock Center for fly stocks, and Developmental Studies Hybridoma Bank for antibodies.

This work is supported by grants from National Institutes of Health (GM061269, GM067045, and GM106188), National Natural Science Foundation of China (31328017), and Welch foundation (I-1603). J. Jiang is a Eugene McDermott Endowed Scholar in Biomedical Science at the University of Texas Southwestern.

The authors declare no competing financial interests.

Submitted: 4 September 2014

Accepted: 28 January 2015

References

Amcheslavsky, A., J. Jiang, and Y.T. Ip. 2009. Tissue damage-induced intestinal stem cell division in *Drosophila*. *Cell Stem Cell*. 4:49–61. <http://dx.doi.org/10.1016/j.stem.2008.10.016>

Amcheslavsky, A., N. Ito, J. Jiang, and Y.T. Ip. 2011. Tuberous sclerosis complex and Myc coordinate the growth and division of *Drosophila*

intestinal stem cells. *J. Cell Biol.* 193:695–710. <http://dx.doi.org/10.1083/jcb.201103018>

- Arimura, S., A. Matsunaga, T. Kitamura, K. Aoki, M. Aoki, and M.M. Taketo. 2009. Reduced level of Smoothened suppresses intestinal tumorigenesis by down-regulation of Wnt signaling. *Gastroenterology*. 137:629–638. <http://dx.doi.org/10.1053/j.gastro.2009.04.059>
- Bach, E.A., L.A. Ekas, A. Ayala-Camargo, M.S. Flaherty, H. Lee, N. Perrimon, and G.H. Baeg. 2007. GFP reporters detect the activation of the *Drosophila* JAK/STAT pathway in vivo. *Gene Expr. Patterns*. 7:323–331. <http://dx.doi.org/10.1016/j.modgep.2006.08.003>
- Beachy, P.A., S.S. Karhadkar, and D.M. Berman. 2004. Tissue repair and stem cell renewal in carcinogenesis. *Nature*. 432:324–331. <http://dx.doi.org/10.1038/nature03100>
- Berman, D.M., S.S. Karhadkar, A. Maitra, R. Montes De Oca, M.R. Gerstenblith, K. Briggs, A.R. Parker, Y. Shimada, J.R. Eshleman, D.N. Watkins, and P.A. Beachy. 2003. Widespread requirement for Hedgehog ligand stimulation in growth of digestive tract tumours. *Nature*. 425:846–851. <http://dx.doi.org/10.1038/nature01972>
- Bielefeld, K.A., S. Amini-Nik, and B.A. Alman. 2013. Cutaneous wound healing: recruiting developmental pathways for regeneration. *Cell. Mol. Life Sci.* 70:2059–2081. <http://dx.doi.org/10.1007/s00018-012-1152-9>
- Biteau, B., and H. Jasper. 2011. EGF signaling regulates the proliferation of intestinal stem cells in *Drosophila*. *Development*. 138:1045–1055. <http://dx.doi.org/10.1242/dev.056671>
- Biteau, B., and H. Jasper. 2014. Slit/Robo signaling regulates cell fate decisions in the intestinal stem cell lineage of *Drosophila*. *Cell Reports*. 7:1867–1875. <http://dx.doi.org/10.1016/j.celrep.2014.05.024>
- Biteau, B., C.E. Hochmuth, and H. Jasper. 2011. Maintaining tissue homeostasis: dynamic control of somatic stem cell activity. *Cell Stem Cell*. 9:402–411. <http://dx.doi.org/10.1016/j.stem.2011.10.004>
- Briscoe, J., and P.P. Thérond. 2013. The mechanisms of Hedgehog signaling and its roles in development and disease. *Nat. Rev. Mol. Cell Biol.* 14:416–429. <http://dx.doi.org/10.1038/nrm3598>
- Buchon, N., N.A. Broderick, S. Chakrabarti, and B. Lemaitre. 2009a. Invasive and indigenous microbiota impact intestinal stem cell activity through multiple pathways in *Drosophila*. *Genes Dev.* 23:2333–2344. <http://dx.doi.org/10.1101/gad.1827009>
- Buchon, N., N.A. Broderick, M. Poidevin, S. Pradervand, and B. Lemaitre. 2009b. *Drosophila* intestinal response to bacterial infection: activation of host defense and stem cell proliferation. *Cell Host Microbe*. 5:200–211. <http://dx.doi.org/10.1016/j.chom.2009.01.003>
- Buchon, N., D. Osman, F.P. David, H.Y. Fang, J.P. Boquete, B. Deplancke, and B. Lemaitre. 2013. Morphological and molecular characterization of adult midgut compartmentalization in *Drosophila*. *Cell Reports*. 3:1725–1738. <http://dx.doi.org/10.1016/j.celrep.2013.04.001>
- Chen, Y., and G. Struhl. 1998. In vivo evidence that Patched and Smoothened constitute distinct binding and transducing components of a Hedgehog receptor complex. *Development*. 125:4943–4948.
- Cordero, J.B., R.K. Stefanatos, A. Scopelliti, M. Vidal, and O.J. Sansom. 2012. Inducible progenitor-derived Wingless regulates adult midgut regeneration in *Drosophila*. *EMBO J.* 31:3901–3917. <http://dx.doi.org/10.1038/emboj.2012.248>
- Fendrich, V., F. Esni, M.V. Garay, G. Feldmann, N. Habbe, J.N. Jensen, Y. Dor, D. Stoffers, J. Jensen, S.D. Leach, and A. Maitra. 2008. Hedgehog signaling is required for effective regeneration of exocrine pancreas. *Gastroenterology*. 135:621–631. <http://dx.doi.org/10.1053/j.gastro.2008.04.011>
- Goulas, S., R. Conder, and J.A. Knoblich. 2012. The Par complex and integrins direct asymmetric cell division in adult intestinal stem cells. *Cell Stem Cell*. 11:529–540. <http://dx.doi.org/10.1016/j.stem.2012.06.017>
- Gu, D., Q. Fan, X. Zhang, and J. Xie. 2012. A role for transcription factor STAT3 signaling in oncogene Smoothened-driven carcinogenesis. *J. Biol. Chem.* 287:38356–38366. <http://dx.doi.org/10.1074/jbc.M112.377382>
- Guo, Z., I. Driver, and B. Ohlstein. 2013. Injury-induced BMP signaling negatively regulates *Drosophila* midgut homeostasis. *J. Cell Biol.* 201:945–961. <http://dx.doi.org/10.1083/jcb.201302049>
- Hsu, Y.C., L. Li, and E. Fuchs. 2014. Transit-amplifying cells orchestrate stem cell activity and tissue regeneration. *Cell*. 157:935–949. <http://dx.doi.org/10.1016/j.cell.2014.02.057>
- Jiang, H., and B.A. Edgar. 2009. EGFR signaling regulates the proliferation of *Drosophila* adult midgut progenitors. *Development*. 136:483–493. <http://dx.doi.org/10.1242/dev.026955>
- Jiang, H., and B.A. Edgar. 2012. Intestinal stem cell function in *Drosophila* and mice. *Curr. Opin. Genet. Dev.* 22:354–360. <http://dx.doi.org/10.1016/j.gde.2012.04.002>
- Jiang, H., P.H. Patel, A. Kohlmaier, M.O. Grenley, D.G. McEwen, and B.A. Edgar. 2009. Cytokine/Jak/Stat signaling mediates regeneration and

- homeostasis in the *Drosophila* midgut. *Cell*. 137:1343–1355. <http://dx.doi.org/10.1016/j.cell.2009.05.014>
- Jiang, H., M.O. Grenley, M.J. Bravo, R.Z. Blumhagen, and B.A. Edgar. 2011. EGFR/Ras/MAPK signaling mediates adult midgut epithelial homeostasis and regeneration in *Drosophila*. *Cell Stem Cell*. 8:84–95. <http://dx.doi.org/10.1016/j.stem.2010.11.026>
- Jiang, J., and C.C. Hui. 2008. Hedgehog signaling in development and cancer. *Dev. Cell*. 15:801–812. <http://dx.doi.org/10.1016/j.devcel.2008.11.010>
- Kapuria, S., J. Karpac, B. Biteau, D. Hwangbo, and H. Jasper. 2012. Notch-mediated suppression of TSC2 expression regulates cell differentiation in the *Drosophila* intestinal stem cell lineage. *PLoS Genet*. 8:e1003045. <http://dx.doi.org/10.1371/journal.pgen.1003045>
- Karpowicz, P., J. Perez, and N. Perrimon. 2010. The Hippo tumor suppressor pathway regulates intestinal stem cell regeneration. *Development*. 137:4135–4145. <http://dx.doi.org/10.1242/dev.060483>
- Lee, T., and L. Luo. 2001. Mosaic analysis with a repressible cell marker (MARCM) for *Drosophila* neural development. *Trends Neurosci*. 24:251–254. [http://dx.doi.org/10.1016/S0166-2236\(00\)01791-4](http://dx.doi.org/10.1016/S0166-2236(00)01791-4)
- Lee, W.C., K. Beebe, L. Sudmeier, and C.A. Micchelli. 2009. Adenomatous polyposis coli regulates *Drosophila* intestinal stem cell proliferation. *Development*. 136:2255–2264. <http://dx.doi.org/10.1242/dev.035196>
- Li, Z., Y. Zhang, L. Han, L. Shi, and X. Lin. 2013. Trachea-derived Dpp controls adult midgut homeostasis in *Drosophila*. *Dev. Cell*. 24:133–143. <http://dx.doi.org/10.1016/j.devcel.2012.12.010>
- Li, Z., Y. Guo, L. Han, Y. Zhang, L. Shi, X. Huang, and X. Lin. 2014. Debra-mediated Ci degradation controls tissue homeostasis in *Drosophila* adult midgut. *Stem Cell Rev*. 2:135–144. <http://dx.doi.org/10.1016/j.stemcr.2013.12.011>
- Madison, B.B., K. Braunstein, E. Kuizon, K. Portman, X.T. Qiao, and D.L. Gumucio. 2005. Epithelial hedgehog signals pattern the intestinal crypt-villus axis. *Development*. 132:279–289. <http://dx.doi.org/10.1242/dev.01576>
- Marianes, A., and A.C. Spradling. 2013. Physiological and stem cell compartmentalization within the *Drosophila* midgut. *eLife*. 2:e00886. <http://dx.doi.org/10.7554/eLife.00886>
- Martín, V., G. Carrillo, C. Torroja, and I. Guerrero. 2001. The sterol-sensing domain of Patched protein seems to control Smoothened activity through Patched vesicular trafficking. *Curr. Biol*. 11:601–607. [http://dx.doi.org/10.1016/S0960-9822\(01\)00178-6](http://dx.doi.org/10.1016/S0960-9822(01)00178-6)
- McGuire, S.E., Z. Mao, and R.L. Davis. 2004. Spatiotemporal gene expression targeting with the TARGET and gene-switch systems in *Drosophila*. *Sci. STKE*. 2004:pl6.
- Micchelli, C.A., and N. Perrimon. 2006. Evidence that stem cells reside in the adult *Drosophila* midgut epithelium. *Nature*. 439:475–479. <http://dx.doi.org/10.1038/nature04371>
- Nakano, Y., I. Guerrero, A. Hidalgo, A. Taylor, J.R. Whittle, and P.W. Ingham. 1989. A protein with several possible membrane-spanning domains encoded by the *Drosophila* segment polarity gene *patched*. *Nature*. 341:508–513. <http://dx.doi.org/10.1038/341508a0>
- Ochoa, B., W.K. Syn, I. Delgado, G.F. Karaca, Y. Jung, J. Wang, A.M. Zubiaga, O. Fresno, A. Omenetti, M. Zdanowicz, et al. 2010. Hedgehog signaling is critical for normal liver regeneration after partial hepatectomy in mice. *Hepatology*. 51:1712–1723. <http://dx.doi.org/10.1002/hep.23525>
- Ohlstein, B., and A. Spradling. 2006. The adult *Drosophila* posterior midgut is maintained by pluripotent stem cells. *Nature*. 439:470–474. <http://dx.doi.org/10.1038/nature04333>
- Ohlstein, B., and A. Spradling. 2007. Multipotent *Drosophila* intestinal stem cells specify daughter cell fates by differential notch signaling. *Science*. 315:988–992. <http://dx.doi.org/10.1126/science.1136606>
- Peng, Y.C., C.M. Levine, S. Zahid, E.L. Wilson, and A.L. Joyner. 2013. Sonic hedgehog signals to multiple prostate stromal stem cells that replenish distinct stromal subtypes during regeneration. *Proc. Natl. Acad. Sci. USA*. 110:20611–20616. <http://dx.doi.org/10.1073/pnas.1315729110>
- Perdigoto, C.N., F. Schweisguth, and A.J. Bardin. 2011. Distinct levels of Notch activity for commitment and terminal differentiation of stem cells in the adult fly intestine. *Development*. 138:4585–4595. <http://dx.doi.org/10.1242/dev.065292>
- Petrova, R., and A.L. Joyner. 2014. Roles for Hedgehog signaling in adult organ homeostasis and repair. *Development*. 141:3445–3457. <http://dx.doi.org/10.1242/dev.083691>
- Ramallo-Santos, M., D.A. Melton, and A.P. McMahon. 2000. Hedgehog signals regulate multiple aspects of gastrointestinal development. *Development*. 127:2763–2772.
- Ren, F., B. Wang, T. Yue, E.Y. Yun, Y.T. Ip, and J. Jiang. 2010. Hippo signaling regulates *Drosophila* intestine stem cell proliferation through multiple pathways. *Proc. Natl. Acad. Sci. USA*. 107:21064–21069. <http://dx.doi.org/10.1073/pnas.1012759107>
- Ren, F., Q. Shi, Y. Chen, A. Jiang, Y.T. Ip, H. Jiang, and J. Jiang. 2013. *Drosophila* Myc integrates multiple signaling pathways to regulate intestinal stem cell proliferation during midgut regeneration. *Cell Res*. 23:1133–1146. <http://dx.doi.org/10.1038/cr.2013.101>
- Scopelliti, A., J.B. Cordero, F. Diao, K. Strathdee, B.H. White, O.J. Sansom, and M. Vidal. 2014. Local control of intestinal stem cell homeostasis by enteroendocrine cells in the adult *Drosophila* midgut. *Curr. Biol*. 24:1199–1211. <http://dx.doi.org/10.1016/j.cub.2014.04.007>
- Shaw, R.L., A. Kohlmaier, C. Polesello, C. Veelken, B.A. Edgar, and N. Tapon. 2010. The Hippo pathway regulates intestinal stem cell proliferation during *Drosophila* adult midgut regeneration. *Development*. 137:4147–4158. <http://dx.doi.org/10.1242/dev.052506>
- Shin, K., J. Lee, N. Guo, J. Kim, A. Lim, L. Qu, I.U. Mysorekar, and P.A. Beachy. 2011. Hedgehog/Wnt feedback supports regenerative proliferation of epithelial stem cells in bladder. *Nature*. 472:110–114. <http://dx.doi.org/10.1038/nature09851>
- Singh, S., Z. Wang, D. Liang Fei, K.E. Black, J.A. Goetz, R. Tokhunts, C. Giambelli, J. Rodriguez-Blanco, J. Long, E. Lee, et al. 2011. Hedgehog-producing cancer cells respond to and require autocrine Hedgehog activity. *Cancer Res*. 71:4454–4463. <http://dx.doi.org/10.1158/0008-5472.CAN-10-2313>
- Sisson, J.C., K.S. Ho, K. Suyama, and M.P. Scott. 1997. Costal2, a novel kinesin-related protein in the Hedgehog signaling pathway. *Cell*. 90:235–245. [http://dx.doi.org/10.1016/S0092-8674\(00\)80332-3](http://dx.doi.org/10.1016/S0092-8674(00)80332-3)
- Staley, B.K., and K.D. Irvine. 2010. Warts and Yorkie mediate intestinal regeneration by influencing stem cell proliferation. *Curr. Biol*. 20:1580–1587. <http://dx.doi.org/10.1016/j.cub.2010.07.041>
- Taipale, J., and P.A. Beachy. 2001. The Hedgehog and Wnt signalling pathways in cancer. *Nature*. 411:349–354. <http://dx.doi.org/10.1038/35077219>
- Tian, A., and J. Jiang. 2014. Intestinal epithelium-derived BMP controls stem cell self-renewal in *Drosophila* adult midgut. *eLife*. 3:e01857. <http://dx.doi.org/10.7554/eLife.01857>
- van den Brink, G.R., S.A. Bleuming, J.C. Hardwick, B.L. Schepman, G.J. Offerhaus, J.J. Keller, C. Nielsen, W. Gaffield, S.J. van Deventer, D.J. Roberts, and M.P. Peppelenbosch. 2004. Indian Hedgehog is an antagonist of Wnt signaling in colonic epithelial cell differentiation. *Nat. Genet*. 36:277–282. <http://dx.doi.org/10.1038/ng1304>
- Varnat, F., A. Duquet, M. Malerba, M. Zbinden, C. Mas, P. Gervaz, and A. Ruiz i Altaba. 2009. Human colon cancer epithelial cells harbour active HEDGEHOG-Gli1 signalling that is essential for tumour growth, recurrence, metastasis and stem cell survival and expansion. *EMBO Mol. Med*. 1:338–351. <http://dx.doi.org/10.1002/emmm.200900039>
- Varnat, F., G. Zaccchetti, and A. Ruiz i Altaba. 2010. Hedgehog pathway activity is required for the lethality and intestinal phenotypes of mice with hyperactive Wnt signaling. *Mech. Dev*. 127:73–81. <http://dx.doi.org/10.1016/j.mod.2009.10.005>
- Wang, G., K. Amanai, B. Wang, and J. Jiang. 2000. Interactions with Costal2 and Suppressor of fused regulate nuclear translocation and activity of Cubitus interruptus. *Genes Dev*. 14:2893–2905. <http://dx.doi.org/10.1101/gad.843900>
- Weston, C.R., and R.J. Davis. 2007. The JNK signal transduction pathway. *Curr. Opin. Cell Biol*. 19:142–149. <http://dx.doi.org/10.1016/j.ccb.2007.02.001>
- Xu, N., S.Q. Wang, D. Tan, Y. Gao, G. Lin, and R. Xi. 2011. EGFR, Wingless and JAK/STAT signaling cooperatively maintain *Drosophila* intestinal stem cells. *Dev. Biol*. 354:31–43. <http://dx.doi.org/10.1016/j.ydbio.2011.03.018>
- Yauch, R.L., S.E. Gould, S.J. Scales, T. Tang, H. Tian, C.P. Ahn, D. Marshall, L. Fu, T. Januario, D. Kallop, et al. 2008. A paracrine requirement for hedgehog signalling in cancer. *Nature*. 455:406–410. <http://dx.doi.org/10.1038/nature07275>
- Zeng, X., C. Chauhan, and S.X. Hou. 2010. Characterization of midgut stem cell- and enteroblast-specific Gal4 lines in drosophila. *Genesis*. 48:607–611. <http://dx.doi.org/10.1002/dvg.20661>
- Zhang, W., Y. Zhao, C. Tong, G. Wang, B. Wang, J. Jia, and J. Jiang. 2005. Hedgehog-regulated Costal2-kinase complexes control phosphorylation and proteolytic processing of Cubitus interruptus. *Dev. Cell*. 8:267–278. <http://dx.doi.org/10.1016/j.devcel.2005.01.001>
- Zhou, F., A. Rasmussen, S. Lee, and H. Agaisse. 2013. The UPD3 cytokine couples environmental challenge and intestinal stem cell division through modulation of JAK/STAT signaling in the stem cell microenvironment. *Dev. Biol*. 373:383–393. <http://dx.doi.org/10.1016/j.ydbio.2012.10.023>